Thesis for the degree of Licentiate of Engineering

Stability and Statistical Analysis of Transient Waves in Fusion Plasmas

Gergő Pokol

CHALMERS

Department of Radio and Space Science
Chalmers University of Technology
Göteborg, Sweden, 2007

Supervisors: Dr. Tünde Fülöp, Chalmers
Dr. Gábor Pór, BME NTI

Stability and Statistical Analysis of
Transient Waves in Fusion Plasmas
Gergő Pokol

Technical Report No. 25L
ISSN 1652-9103
Nonlinear Electrodynamics Group
Department of Radio and Space Science
Chalmers University of Technology
SE–412 96 Göteborg
Sweden
Telephone +46–(0)31–772 10 00

Printed in Sweden by
Reproservice
Chalmers Tekniska Högskola
Göteborg, Sweden, 2007

Stability and Statistical Analysis of
Transient Waves in Fusion Plasmas

Gergő Pokol
Department of Radio and Space Science
Chalmers University of Technology

Abstract

Thermonuclear energy generation in magnetically confined plasmas offers an appealing energy source for coming generations. Some of the still unsolved problems in fusion plasma physics involve plasma transport and stability of plasma waves. Two such problems are addressed in the present thesis.

Transient magnetohydrodynamical (MHD) modes were typically detected on the Wendelstein 7-AS stellarator in correlation with transient transport events, called ELM-like modes. The temporal and spatial structure of these transient modes are analysed in the thesis using custom developed methods based on Mirnov-coil and lithium beam emission spectroscopy measurements. The statistical connection between the power modulation of transient MHD modes and the temporal changes of electron transport related quantities is investigated and possible theoretical explanations are proposed.

Runaway electrons already pose serious problems in connection with disruptions in present-day tokamak-type fusion devices, and the problems are expected to become even more severe in next generation machines, like ITER. There are still discrepancies between the theoretical understanding and experimental results concerning the generation of runaway electrons, some of which might be explained by an interaction between the runaway electron beam and plasma waves. Linear and quasi-linear evolution of magnetosonic-whistler waves excited by runaway electrons is considered in the thesis, and it is shown that these waves can indeed be destabilized and can scatter resonant electrons from the beam.

Keywords: fusion plasma physics, stellarator, transient MHD mode, transient transport, wavelet transform, short-time Fourier transform, tokamak disruption, runaway electron, whistler wave, quasi-linear diffusion

Publications

[A] G. Pokol, G. Por, S. Zoletnik and W7-AS team, "Application of a bandpower correlation method to the statistical analysis of MHD bursts in quiescent Wendelstein-7 AS stellarator plasmas", Plasma Physics and Controlled Fusion **49**, 1391-1408 (2007).

[B] G. Pokol, G. Por, S. Zoletnik, N. P. Basse and W7-AS team, "Amplitude correlation analysis of W7-AS Mirnov-coil array data and other transport relevant diagnostics", Proc. of 20th IAEA Fusion Energy Conference, Vilamoura, 2004, (IAEA Conference & Symposium Papers, 2005), Vol. **25/CD**, PS-EX/P6-22 (2005).

[C] G. Pokol, G. Papp, G. Por, S. Zoletnik, A. Weller and W7-AS team, "Experimental study and simulation of W7-AS transient MHD modes", Proc. of PLASMA 2007 International Conference on Research and Applications of Plasmas, Greifswald, 2007, (to be published in the AIP Conference Proceedings Series) TuP31 (2007).

[D] T. Fülöp, G. Pokol, P. Helander and M. Lisak, "Destabilization of magnetosonic-whistler waves by a relativistic runaway beam", Physics of Plasmas **13**, 062506 (2006).

[E] G. Pokol, T. Fülöp and M. Lisak, "Quasi-linear analysis of whistler waves driven by relativistic runaway beams in tokamaks" (to be submitted for publication)

Futher publications
(not included in the thesis)

[X] E. Belonohy, G. Papp, G. Pokol, K. McCormick, S. Zoletnik and W7-AS team, "Systematic Study of Anomalous Transport Events on the W7-AS Stellarator - Quasi-Coherent Mode in the High Density H-Mode Regime", Proc. of PLASMA 2007 International Conference on Research and Applications of Plasmas, Greifswald (to be published in the AIP Conference Proceedings Series) Tu1-3 (2007).

[X] I. Pusztai, D. Dunai, G. Pokol, G. Por, J. Schweinzer and S. Zoletnik, "Capabilities of alkali Beam Emission Spectroscopy for density profile and fluctuation measurements", Proc. of 34th EPS Conference on Plasma Physics, Warsaw, P2.137 (2007).

[X] E. Belonohy, A. Bencze, G. Papp, G. Pokol, K. McCormick, S. Zoletnik and W7-AS team, "Systematic Density Fluctuation Study on W7-AS", Proc. of 34th EPS Conference on Plasma Physics, Warsaw, P2.046 (2007).

[X] G. Papp, G. Pokol, G. Por, S. Zoletnik and W7-AS team, "Investigation of transient MHD modes of Wendelstein 7-Advanced Stellarator", Proc. of International Youth Conference on Energetics, Budapest, 109 (2007).

[X] G. Pokol, T. Fülöp, P. Helander and M. Lisak, "Destabilization of magnetosonic-whistler waves by a relativistic runaway beam", Proc. of 21st IAEA Conference, Chengdu, (Fusion Energy 2006), Vol. **IAEA-CN-149**, TH/P6-2 (2006).

[X] G. Pokol, G. Por, "ALPS loose parts monitoring system and wavelet analysis", International Journal of Nuclear Energy Science and Technology **2**, 241 (2006).

[X] T. Fülöp, G. Pokol, P. Helander and M. Lisak, "Destabilization of magnetosonic-whistler waves by a relativistic runaway beam", Proc. of 33rd EPS Conference on Plasma Physics, Rome, P1.182 (2006).

[X] G. Papp, G. Pokol, G. Por, S. Zoletnik and W7-AS team, "Analysis of transient MHD modes of Wendelstein 7-AS by coherence techniques", Proc. of 32nd EPS Conference on Plasma Physics, Tarragona, P-5.021 (2005).

[X] S. Zoletnik, N. P. Basse, A. Bencze, D. Dunai, M. Hirsch, G. Pokol and G. Por, "Anomalous transport events in the core plasma of the Wendelstein 7-AS stellarator", Proc. of 32nd EPS Conference on Plasma Physics, Tarragona, P-5.023 (2005).

[X] G. Pokol and G. Por, "ALPS loose parts monitoring system and wavelet analysis", Proc. of 29th IMORN International Meeting On Reactor Noise, Budapest, (2004).

[X] G. Pokol, G. Por, S. Zoletnik, E. Fekete, A. Werner and W7-AS team, "Statistical analysis of experimentally observed transient MHD modes", Proc. of 30th EPS Conference on Controlled Fusion and Plasma Physics, St. Petersburg, P-3.7 (2003).

Contents

Acknowledgements

I would like to thank my supervisors, Tünde Fülöp and Gábor Pór, for guiding and encouraging me, and doing all kinds of other things that good supervisors do. I would also like to thank all my colleagues at BME NTI and RSS Chalmers, in particular professors Mietek Lisak and Dan Anderson, for creating an inspiring atmosphere and helping me out with all the problems of everyday research. Especially, computer support provided by Ulf Jordan, Pontus Johannisson and Tobias Hansson made my life much easier. I am grateful to the people of the plasma physics group at KFKI-RMKI for making me feel like a member of their group. I particularly owe a lot to Sándor Zoletnik, who sometimes acted like my third supervisor. I would like to thank the members of the W7-AS team in Greifswald for showing continuing interest in my work, in particular Arthur Weller, who was my host in Greifswald during the most progressive week of my research. I wish to thank members of the international fusion community: Guido Huysmans, Vladym V. Lutsenko, Yurij V. Yakovenko, Sergei Sharapov, Friedrich Wagner, Kent McCormick and many others, for the frank stimulating discussions. Last but not least, I would like to thank my parents for their support, and my little family, Eszter and Emese, for keeping me company throughout this long journey.

Chapter 1

Introduction

As the world is approaching a global energy and environmental crisis, the search for alternative, environmentally friendly energy sources intensifies. The most promising candidate for the basic energy source of the future is the utilization of energy released during fusion of light atomic nuclei [1]. While having all the positive properties of traditional fission energy, it also promises to eliminate some basic problems that fission energy is facing, the most important ones being the highly toxic nuclear waste of fission products and nuclear safety issues.

Fusion produces most of the energy of the Universe, yet it has proved to be extremely difficult to implement controlled fusion power generation on Earth. The main problem is posed by the extremely high temperature (more then 100 million K) needed to overcome the Coulomb repulsion of the nuclei to be fused. Matter at this temperature is in the plasma state and can not be held together by any kind of traditional vessel wall. There are three basic concepts to confine a fusion plasma: gravitational, inertial, and magnetic confinement. Gravitational confinement works only on the scale of stars [2], and the miniature hydrogen bombs of inertial confinement raises questions of practicality [1]. It is commonly believed today that magnetic confinement fusion may be the best solution [3].

The two most successful magnetic confinement device types of present days are the tokamak and the stellarator [1]. Figure 1.1 shows that both use a strong magnetic field (2-8 T) bent to a torus shape and twisted helically to avoid particle losses due to motion along field lines and drifts. The main difference between the two device types is that in stellarators the geometry of the magnetic field is determined by external coils, while tokamaks have a large toroidal plasma current (1-10 MA) giving

the twist to the magnetic field lines, which allows a simpler, toroidally symmetric coil structure.

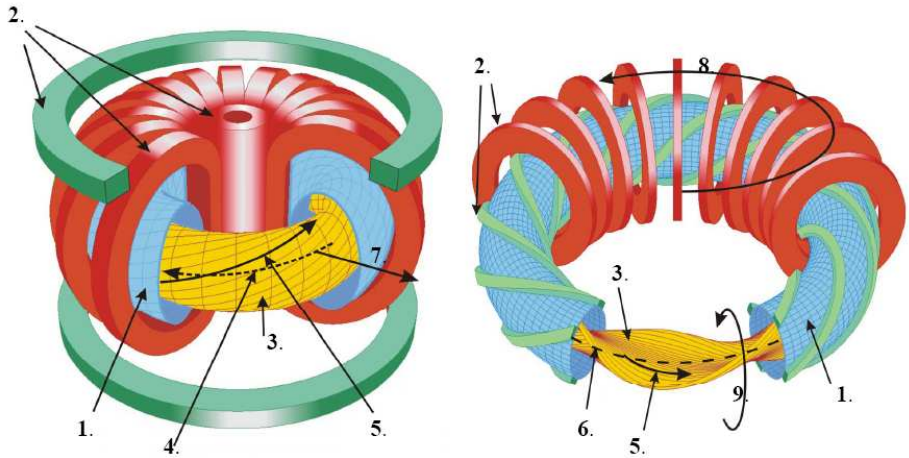

Figure 1.1: Schematic figure of the tokamak (left) and the stellarator (right): 1.-vacuum chamber, 2.-magnetic coils, 3.-plasma, 4.-plasma current, 5.-helically twisted magnetic field line, 6.-magnetic axis, 7.-radial direction, 8.-toroidal direction, 9.- poloidal direction

Research devoted to stellarators and tokamaks is intensive, as new devices are being built around the world to explore operational regimes closer to the electric power producing reactor scale. In the stellarator direction the superconducting W7-X reactor is being built in Greifswald, Germany [4] along with some compact stellarators in the USA [5, 6]. These stellarators are still plasma physics experiments, but the tokamak concept has evolved one step further. The ITER tokamak being built in Cadarache, France, in worldwide cooperation aims to explore reactor relevant operating conditions and to test reactor elements [7].

Although theory is well established in many fields of plasma physics, there are still plenty of open questions to be resolved. Some of the most important issues are from the area where the field of plasma transport theory meets the field of stability of plasma waves. This thesis attempts to tackle two such issues.

It has been observed in many experiments, both in tokamaks [8] and stellarators [9], that transport coefficients change significantly in the proximity of rational surfaces, where the magnetic field lines close on themselves after a few turns. Here, the rotational transform (ι), which is the ratio of the number of poloidal turns to the number of toroidal turns

of a field line, is a low order rational number. The W7-AS stellarator is very much suited for the study of this phenomenon, as it has an almost flat ι-profile [9], so the presence of a rational surface causes a change in the global confinement properties. In contrast, tokamaks have steep ι-profiles, so the change is localized to the proximity of the rational surface. This confinement change is not fully understood, but it is clear that transient transport events, called ELM-like events on W7-AS [10], play a role in it. ELM-like modes were found to be accompanied by transient magnetohydrodynamical (MHD) modes detected as bursts of coherent density and magnetic fluctuations lasting only for a few periods [11]. In the first part of the thesis, we study and model these transient magnetic fluctuations in order to understand the underlying transient transport phenomena.

The other topic covered in the thesis is that of runaway electrons, which is a special effect of collisional transport in plasmas. It emerges from the fact that the drag force experienced by a sufficiently high energy electron decreases with increasing velocity due to the nature of Coulomb collisions of charged particles in plasmas. This implies that above a critical electric field parallel to the magnetic field, there exists a velocity above which the electrostatic accelerating force on the electron overcomes the collisional drag, and electrons continue to be accelerated to relativistic velocities. This critical electric field, E_c, has to be calculated by taking into account the relativistic effects experienced by high speed electrons [12] and is given by

$$E_c = \frac{m_e c}{e\tau_e}, \tag{1.1}$$

where m_e is the electron rest mass, c is the speed of light in vacuum, e is the electron charge, $\tau_e = 4\pi\epsilon_0^2 m_e^2 c^3 / n_e e^4 \ln\Lambda$ is the electron collision time and $\ln\Lambda$ is the Coulomb logarithm. In today's tokamaks, conditions necessary for runaway production seldom arise. They appear typically in non-operational plasma conditions, e.g. in disruptions, when plasma confinement is suddenly lost and the self-inductance of the rapidly cooling plasma gives rise to huge electric fields. The high current, high energy beam of runaway electrons can damage the equipment [13], so understanding their generation and mitigation is of primary importance. Plasma waves can be excited by the anisotropy of the distribution function of runaway electrons, and consequently the waves can affect the generation of runaway electrons, which might explain some experimental observations [14, 15].

The rest of the thesis is organized as follows: The basics of the statistical analysis used on experimental data of W7-AS are summarized in Chapter 2 with a short summary of the experimental results and the proposed physical models. An introduction to the runaway electron phenomenon is given in Chapter 3. The elements of kinetic theory describing wave-particle interaction are introduced in Chapter 4. Finally, a summary and an outlook is given in Chapter 5.

Chapter 2

Statistical analysis

Complex nonlinear systems, like magnetically confined plasmas, show transient phenomena even in quasi-stationary states. Experimental study of these phenomena requires special signal processing tools. In Section 2.1, a family of such tools is introduced, while in Section 2.2 the methods are applied to W7-AS diagnostic signals with the aim to study the transient MHD activity linked to intermittent transport.

2.1 Signal analysis methods for transient signals

The most widely used methods of signal analysis have been developed for stationary time signals, the basic properties of which remain constant for a long time duration in the statistical sense. Many of these methods operate with long-time averages as a basic tool. However, this tool can not be used for the analysis of transient signals, as it would average out the changing properties of the signal. The most important consideration is to avoid introducing artificial effects to the signal resulting from the signal processing. To fulfill this requirement, one should always use time shift invariant transforms and filters: time shift in the input results in the same shift of the output.

Requiring time shift invariance from transforms and filters demands dusting off an old approach. Historically, continuous transforms were the first to be applied [16]. They could be calculated analytically or with the help of analytical computers with ease. Discrete techniques (e.g. FFT) started to emerge, when digital computers appeared. Continuous techniques were discretized with the aim to reduce the number of calculation

steps as much as possible. Doing so, they have lost the shift invariant properties of continuous transforms, which posed no problems for the most frequently analysed stationary time signals, but can be a problem for transient signals. However, continuous transforms can be discretized in a more redundant way, which preserves the shift invariance properties of the original transform, at least to the resolution of the discrete time signal itself [18]. Calculation of transforms with this type of discretization demands an order of magnitude more computation power, but in return they can be used for the analysis of transient signals. To distinguish between the two types of discretizations, the later one is called continuous, reflecting the idea that it preserves the properties of the real continuous transforms.

The signal processing techniques used in this thesis are based on continuous linear time-frequency transforms. One of the main goals of time-frequency transforms is to visualize the temporal changes of frequency content of the signal. The time-frequency plane cannot be mapped with arbitrary precision, as there exists a basic time-frequency unit, the time-frequency atom, which can not be divided further. The minimum extent of the atom is given by Heisenberg's uncertainty principle. The concept of signals being composed of time-frequency atoms was developed as modern communication theory matured [16]. Although some new tools have been developed recently based on specific models of the signals [19], we have chosen to use linear time-frequency transforms, because of their clarity, lack of artifacts, and general applicability [18].

Linear time-frequency transforms (T) of a real signal (x) are calculated by correlating the signal to a family of time-frequency atoms covering the whole time-frequency plane.

$$Tx(u,\xi) = \langle x, g_{u,\xi} \rangle = \int_{-\infty}^{+\infty} x(t) g_{u,\xi}(t) dt, \tag{2.1}$$

where $g_{u,\xi}(t)$ is a time-frequency atom which is a function of time, whose energy is well localized in both time and frequency and $\|g_{u,\xi}(t)\| = 1$. Here, u and ξ are the time and frequency indices of the atom identifying its position on the time-frequency plane.

Linear time-frequency transforms (2.1) of real signals are complex-valued two-parameter functions on the time-frequency plane symmetrical in magnitude across the zero frequency line and anti-symmetric in phase. The squared magnitude of the transform characterises the energy content of the signal, and so the energy-density distribution can be

calculated:

$$P_T x(u,\xi) = |Tx(u,\xi)|^2 . \tag{2.2}$$

The first variant of the continuous linear time-frequency transforms is the short-time Fourier transform (STFT) [16, 18]. In this transform the time-frequency atom family is generated by shifting an atom in time and frequency. For historical reasons, it also involves the modification of the phase by $e^{i\xi u}$:

$$g_{u,\xi}(t) = e^{i\xi t} g(t-u), \tag{2.3}$$

where u is the time-shift and ξ is the frequency-shift of the $g(t)$ normalized window function. In order to produce the shift invariance property of the continuous transforms, u and ξ are dense everywhere on the part of the time-frequency plane limited by the temporal duration of the signal and its Nyquist frequency (half the sampling frequency). Invariance properties of the transform reflect those of the atoms: it is time shift and frequency shift invariant.

A more recent variant of the continuous linear time-frequency transforms is the continuous wavelet transform (CWT) [17, 18] using analytical wavelets. In this transform the time-frequency atom family is generated by shifting an atom in time and scaling it:

$$g_{u,\xi}(t) = \frac{1}{\sqrt{s}} \Psi\left(\frac{t-u}{s}\right), \quad s = \frac{\nu}{\xi}, \tag{2.4}$$

where u is the time-shift, s is the scale parameter, $\Psi(t)$ is an analytical mother wavelet, $\nu = 1/2\pi \int_0^\infty \omega \left|\hat{\Psi}(\omega)\right|^2 d\omega$ is the central frequency of the mother wavelet and $\hat{}$ denotes Fourier transform. The parameters u and s are scanned continuously to give a dense coverage of the part of the time-frequency plane limited by the temporal duration of the signal and its Nyquist frequency. This transform is time shift and scale invariant. Selection between the two transforms must be based on the invariance property required.

The energy-density distributions (2.2) calculated from STFT and CWT are called spectrogram and scalogram respectively. These figures are most often used to visualize the time-frequency evolution of the signal, but instantaneous amplitudes and frequencies of modes can also be extracted quantitatively [18], which can be the basis of further processing. Paper A presents such a technique, where the energy-density distribution (spectrogram in this case) is integrated in a frequency range giving the bandpower approximating the power content of a given mode.

Conclusions are drawn from the cross-correlation functions calculated between bandpowers at different frequencies. This technique is called the bandpower correlation method.

While energy-density distributions are very important, information in the phase of the transforms should not be omitted. Phase information is particularly valuable, if we can compare two signals (x and y) having a component of common origin. Then their relative phase

$$\Theta_{x,y}(u,\xi) = \arg\left(Tx(u,\xi)\overline{Ty(u,\xi)}\right), \tag{2.5}$$

where $\overline{T}$ denotes the complex conjugate of T, can reveal either the spatial structure or the propagation speed of the perturbations.

If we have a probe array (consisting of N probes) covering the whole spatial extent of the perturbation with sufficient spatial resolution, we can reconstruct the spatial structure of the perturbation using the relative phases between the signals. As the phase is additive, the number of independent estimates in this method is equal to N. The reliability of this method can be improved by smoothing the cross-transform values in time, thus averaging independent measurements:

$$\langle Tx(u,\xi)\overline{Ty(u,\xi)}\rangle = \left[Tx(u,\xi)\overline{Ty(u,\xi)}\right] * A(u,\xi), \tag{2.6}$$

where $*$ denotes convolution in time and $A(u,\xi)$ is a convolution kernel chosen to preserve the invariance properties of transform T. This way, time shift invariance is preserved by choosing to average by convolution smoothing. A frequency shift invariant convolution kernel $A(u)$ preserves frequency shift invariance for STFT and an affine invariant kernel preserves affine invariance of CWT. This smoothing degrades the temporal resolution of the method, so the length of the smoothing kernel has to be set as a compromise between the temporal resolution and the suppression of independent noise terms. An additional effect of the smoothing is that the independent noise terms cancel out differently for each pair of signals, so the number of quasi-independent measurements of relative phases in this case is $N(N-1)/2$.

Tuning the method above requires us to know the relative strength of the common component in the signals, which can be characterized by the coherence:

$$COH_{x,y}(u,\xi) = \frac{\left|\langle Tx(u,\xi)\overline{Ty(u,\xi)}\rangle\right|}{\sqrt{\langle P_T x(u,\xi)\rangle\langle P_T y(u,\xi)\rangle}}, \tag{2.7}$$

which is the magnitude of the cross-transform normalized by the smoothed energy-density distributions of the two signals. The reliability of the coherence estimation largely depends on the length of the smoothing: without smoothing we get $COH_{x,y}(u,\xi) = 1$, and with increasing the number of independent measurements averaged $COH_{x,y}(u,\xi) \to 0$ at time-frequency areas, where no common component is present. Weaker common signal components (in comparison with the independent noise components) have lower coherence value and thus need longer averages to stand out.

2.2 Analysis of W7-AS transient events

The signal analysis methods presented in Section 2.1 can be used for a wide variety of signals. In this section, applications presented in papers A, B and C are summarized shortly.

The W7-AS stellarator was quite well equipped with diagnostics, but not all were capable of fluctuation measurements. In this thesis an analysis utilizing Mirnov coil, Lithium beam emission spectroscopy (LiBES), collective laser scattering (LOTUS) and electron-cyclotron emission spectroscopy (ECE) signals is presented.

The main diagnostic used in this thesis is the Mirnov coil. This is a small coil measuring changes in the poloidal magnetic field. These coils are usually organized in arrays, so that they can measure the spatial structure of the magnetic perturbations. Figure 2.1 shows the positions of the poloidal array MIR-1 [20] and the toroidal array MIR-354 used in the analysis. The most important problem with the interpretation of Mirnov coil measurements is that they are not well-localized.

Our second diagnostic, the LiBES provides point measurement of electron density and its fluctuation [11]. The basic setup of the diagnostic is shown on Figure 2.2. The measurement principle is the following: a high energy Li atomic beam penetrates the plasma and the electrons of the atom are excited through collisional processes, mainly electron impact excitation. The characteristic photons emitted during the spontaneous de-excitations are detected. The intersection of the line of sight of the detector and the beam gives the measurement point. The problem is that beam atoms also get ionized, so that they are lost from the beam. This process limits the applicability of this measurement to the edge region of the plasma.

The most novel diagnostic, the LOTUS system, is dedicated to the

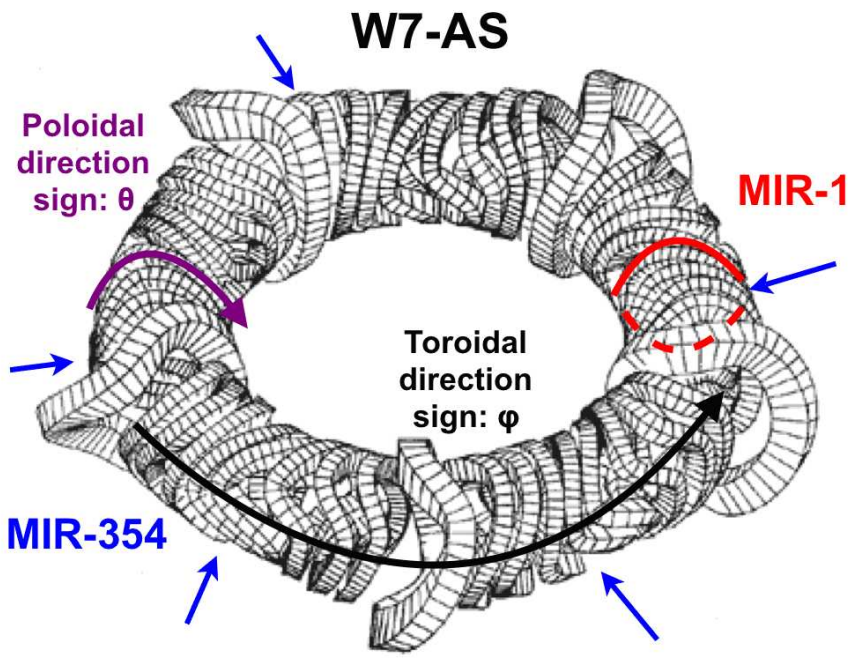

Figure 2.1: Modular magnetic coils of the W7-AS stellarator with the positions of the MIR-1 poloidal and the MIR-354 toroidal Mirnov coil arrays

measurement of millimetre scale electron density turbulence responsible for the anomalous transport [21]. The idea is that a laser beam shot through the plasma scatters on the grating formed by electron density waves with wavelength of the order of millimeters. This diagnostic signal is used in the thesis to characterize the strength of the micro-turbulence.

The ECE diagnostic measures the intensity of the electron-cyclotron radiation in narrow frequency bands separately. Each frequency identifies the flux surface of its source through the strength of the local magnetic field. This diagnostic provides a local electron temperature measurement [10].

The most thoroughly analysed phenomena in this thesis are the transient transport events (ELM-like modes [10]) and the transient MHD modes connected to them in the confinement transition in the W7-AS stellarator around the 1/3 edge rotational transform [9]. This transition is thought to be the manifestation of the rotation transform sensitivity of

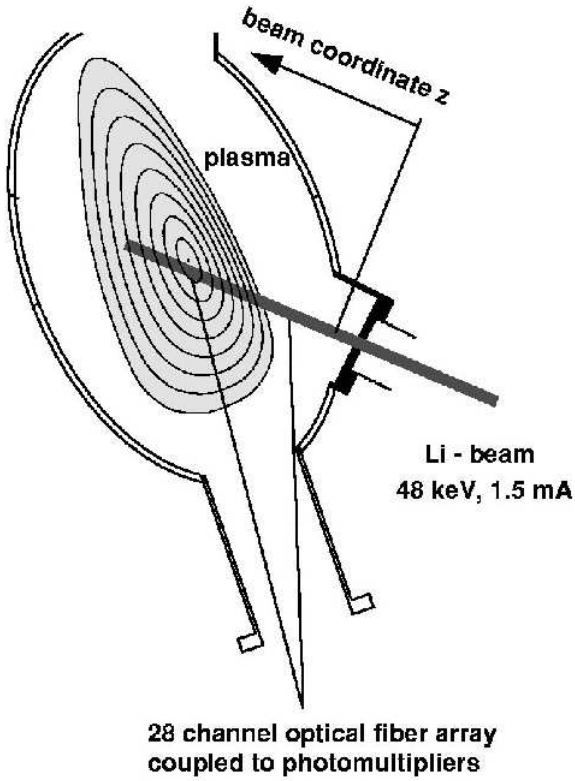

Figure 2.2: Schematic drawing of the LiBES diagnostic of W7-AS

the anomalous transport phenomena, which has also been documented in tokamak type devices [8]. There is a gradual change by a factor of 2 in energy confinement time in response to a small change of 0.02 of the rotational transform at the plasma edge. An experimental study of this transition was carried out by processing magnetic fluctuation signals of the poloidal and toroidal Mirnov-coil arrays of W7-AS and comparing these signals to other transport relevant diagnostics mentioned above.

Discharges analysed are pure electron-cyclotron resonance heated (ECRH) discharges, so there are neither fast ions (such as in [22]) nor steep pressure gradients available to drive MHD modes. Nevertheless, transient MHD modes lasting only for a few periods could be observed in both the magnetic fluctuations measured by Mirnov coils and edge density fluctuations measured by LiBES [11]. Although, the frequency of the individual transients could change, they were organized around

characteristic frequencies [23]. They were rotating in the electron diamagnetic drift direction and could have a poloidal structure [24]. A direct link between the anomalous transport and transient MHD modes is proved by the observation that the changes in the root mean square (RMS) amplitude of the Mirnov coil signals correlated in the 100 μs time scale to the modulation of the intensity of the microturbulence measured by LOTUS [25].

Paper A presents the bandpower correlation analysis of signals of the MIR-1 array for an experiment series consisting of discharges of four densities from both sides of the aforementioned confinement transition around the 1/3 edge rotational transform value (shot numbers 52123-52175). The general conclusion is that correlation between the power modulation of fluctuations with different frequencies was found to be strong in 'bad confinement' plasmas and insignificant in the statistical sense in 'good confinement' plasmas. According to our hypothesis, different characteristic frequencies of the modes can be linked to different radial localization through the radial variation of the poloidal flow velocity. This statement is verified by the observation that during a slow transition from 'good confinement' to 'bad confinement' the characteristic frequencies were changing gradually, and slower flow velocities resulted in lower frequencies [23]. This way, different frequencies indicate phenomena at different radial locations, and stronger correlation between them means radially extended structures.

Paper B extends the analysis to the LiBES and LOTUS diagnostics mentioned in the first part of the section. A slow current ramp shot (number 47940) is analysed in detail. This shot shows a gradual change from 'good confinement' to 'bad confinement', and has both MIR-1, LiBES and LOTUS data available for comparison. Cross-correlation functions calculated between Mirnov coil signals and a selected LiBES channel showed the spatiotemporal structure of the transient MHD modes. In order to examine the link between the power variation of transient MHD modes, electron density profile modulations and the intensity of the microturbulence, bandpowers produced from Mirnov-coil signals have also been correlated to LiBES signals and a selected LOTUS bandpower, respectively. Significant correlations were found only in the 'bad confinement' states, indicating strong transient transport activity.

Correlations were found between Mirnov coil bandpowers and transient flattenings in the electron temperature profile measured by ECE. This time significant, although smaller, correlation was found in 'good

confinement' states also. This is an important finding, as it proves a direct link between transient MHD modes and transient transport events. This analysis is not included in the thesis, but in references [26] and [27].

Paper C deals with the spatial structure of the transient MHD modes determined using methods based on the relative phases (2.5) of STFT (2.3) and CWT (2.4). The main result of this analysis is that besides the coherent transient MHD modes with spatial structure $(n, m) = (1, 1/\iota)$, there are other transient modes with low poloidal mode numbers. These modes do not have such a high coherence on the long term, so they were not detected by previous methods using long-time averages.

There are two possible explanations to the strong correlation between transient transport and transient MHD modes: either an MHD instability is causing the rapid radial transport, or the other way around.

Regarding the first possibility, the instability is probably destabilized at some critical value of a quantity related to transport processes (temperature gradient, plasma rotation velocity, etc...), and causes transport through nonlinear processes. The mode disappears as soon as the driving term vanishes.

Regarding the second possibility, one variation to the sequence of events could be the following: The starting point is the opening of some poloidally localized radial transport channel (e.g. L-mode filamentary structures [28]). Through this channel, hot and dense plasma is injected into a flux tube on an outer flux surface and moves the plasma out of force balance. This would trigger an MHD wave as a harmonic response of the plasma predominantly with $(n, m) = (1, 1/\iota)$, but Alfvén eigenmodes [22, 29] with other spatial structures are also possible. The density on the flux surface equilibrates quickly and the transient MHD mode is damped.

Another way, in which transport could cause rotating harmonic structures with $(n, m) = (1, 1/\iota)$, is based on the spreading of the current perturbations caused by macroscopic events of drift-Alfvén turbulence along magnetic field lines [24].

Independent on the direction of causality, our results fit well into the picture: in 'bad confinement' conditions multiple frequency MHD modes are modulated in a correlated way, meaning a radially extended perturbation to the plasma. In 'good confinement', modes at different frequencies are modulated in an uncorrelated way, therefore the perturbation in the plasma should be more localized. This difference on the radial extent of the perturbation was also seen in the correlation analysis

of electron cyclotron emission (ECE) temperature measurements [26].

Chapter 3

Runaway electrons in disruptions

Disruptions occur when operational limits of a tokamak are tested and can impose enormous stresses on the plasma facing components, the vacuum vessel, and all in-vessel components.

When the plasma reaches a stability limit, suddenly a large particle and heat flux reaches the first wall resulting in sputtering and influx of wall particles. If the impurities penetrate deep enough, the Bremsstrahlung of the relatively heavy impurity ions quickly radiates off practically the whole plasma energy, and a disruption occurs. During this thermal quench, the plasma temperature falls to a few eVs typically within 1 ms, and causes the resistivity parallel to the magnetic field to increase dramatically, as $\eta_{\|} \propto T^{-3/2}$ [12]. Due to the self-inductance of the plasma, the current quench time needed for the toroidal current to decay is significantly longer than the thermal quench time (10 ms or more). Large currents flowing in a medium with high resistivity result in high electric fields according to Ohm's law. This can lead to generation of runaway electrons that may damage the first wall. This problem is addressed in papers D and E.

3.1 Basic equations of the kinetic theory of plasmas

The mathematical treatment of runaway electrons is possible through the kinetic theory of plasmas. If the number of charged particles of species "s" is conserved in a plasma, the distribution function of the

species $f_s(\mathbf{r}, \mathbf{v}, t)$ obeys the Vlasov equation

$$\frac{\partial f_s}{\partial t} + \mathbf{v} \cdot \nabla f_s + \frac{e_s}{m_s}(\tilde{\mathbf{E}} + \mathbf{v} \times \tilde{\mathbf{B}}) \frac{\partial f_s}{\partial \mathbf{v}} = 0, \tag{3.1}$$

where e_s and m_s are the charge and the mass of the particle respectively, and $\tilde{\mathbf{E}}$ and $\tilde{\mathbf{B}}$ are the electric and the magnetic fields. These electric and magnetic fields include the small-scale (less then the Debye length) fluctuations responsible for interaction of individual particles. If we detach the effects of the small-scale fluctuations, and include them in a separate collision operator $C_s(f_s)$, we arrive at the Boltzmann equation

$$\frac{\partial f_s}{\partial t} + \mathbf{v} \cdot \nabla f_s + \frac{e_s}{m_s}(\mathbf{E} + \mathbf{v} \times \mathbf{B}) \frac{\partial f_s}{\partial \mathbf{v}} = C_s(f_s), \tag{3.2}$$

which now includes only the $\mathbf{E}$ and $\mathbf{B}$ macroscopic average electric and magnetic fields explicitly. All quantities included in the Boltzmann equation can be measured, and it is the basic equation of the kinetic theory.

In some cases – usually in the description of processes involving shorter time scales than the characteristic collision times – the $C_s(f_s)$ collision term can be omitted, and the Boltzmann equation (3.2) takes the form of the Vlasov equation (3.1).

3.2 Runaway electron generation

For Coulomb collisions in plasmas the collision operator in the kinetic equation (3.2) can be modelled by the Fokker-Planck operator. Finding a suitable approximation of the Fokker-Planck operator is a complex topic [12]. Only one aspect of it is introduced in this section, which is essential for the understanding of the generation of runaway electrons.

Figure 3.1 shows the friction force experienced by an electron as a function of its kinetic energy. As faster electrons spend less time in the Debye sphere of other electrons, above a critical energy the friction force decreases. The maximum of the function is located at about the thermal energy level T_e, and the electric field (parallel to the magnetic field in magnetized plasmas) needed to overcome the maximum friction force is the Dreicer field

$$E_D = \frac{n_e e^2 \ln \Lambda}{4\pi\epsilon_0^2 T_{eV}}, \tag{3.3}$$

where n_e is the electron density, e is the electron charge, $\ln \Lambda$ is the Coulomb logarithm (usually in the range of $10 - 20$) [12] and T_{eV} is the

electron temperature measured in electronvolts. According to relativistic calculations, the friction force also has a minimum as the kinetic energy reaches the rest energy. The minimum electric field needed to overcome friction is the critical field

$$E_c = \frac{n_e e^3 \ln \Lambda}{4\pi\epsilon_0^2 m_e c^2}. \tag{3.4}$$

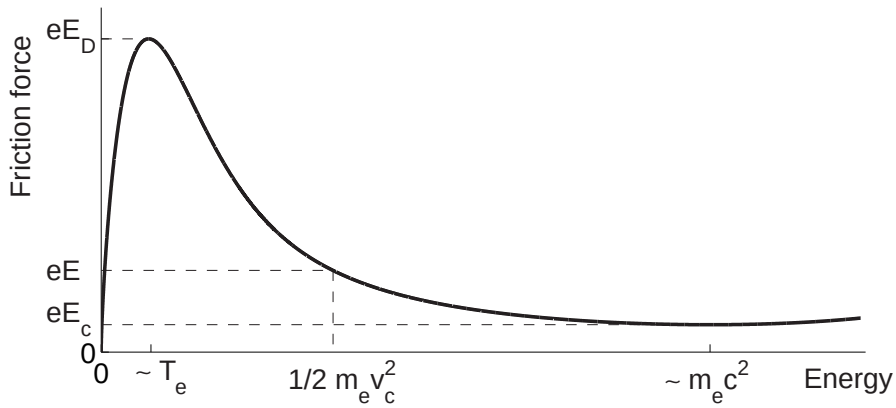

Figure 3.1: A sketch of the friction force as a function of electron energy (reproduced with permission from author [30])

Primary generation of runaway electrons may occur through the Dreicer mechanism or the "burst" mechanism. Dreicer generation works in quasi-steady states, when an electric field larger than the critical field exists $E_\parallel > E_c$. In this mechanism the tail of the Maxwell distribution of plasma electrons becomes runaway above a critical velocity determined by the electric field according to Figure 3.1. The tail of the thermal electron distribution function lost to the runaway electrons is continuously recovered by the collisional processes leading to a continuous influx to the runaway region. In tokamak disruptions, however, the plasma parameters are far from being quasi-steady. In a rapidly cooling plasma, the electrons originally having lower energy lose their energy faster due to their higher collision frequency. This leads to an electron distribution function having a more pronounced tail than a Maxwellian. If the electric field is sufficiently high, this whole tail can become runaway during the thermal quench [30].

Although primary generation is clearly necessary to start the process, in large tokamak disruptions secondary generation by the avalanche

mechanism quickly takes over, and finally produces the largest fraction of runaway electrons. The elementary process of the avalanche mechanism is a close collision between a high energy runaway electron and a thermal electron, as after the collision both electrons may end up having kinetic energy above the critical one. In the relatively simple disruption model used in Papers D and E, the electric field is constant in time leading to an exponentially growing number of secondary generated runaway electrons [31]. The high electric field ($E_{\|} \gg E_c$) results in a beam-like velocity distribution of the runaway electrons having an order of magnitude higher momentum parallel to the magnetic field than perpendicular to it.

Chapter 4

Wave-particle interaction

The description of plasma waves is often based on the fluid theory, which can be derived from Maxwell's equations and moments of the Boltzmann equation (3.2). The modeling of resonant wave-particle interaction, however, requires elements of the kinetic theory introduced in Section 3.1. Properties of plasma waves can be directly calculated using the kinetic theory, so formulation of the fluid equations will be omitted in this summary.

4.1 Dispersion relation of the magnetosonic-whistler wave

Based on the Maxwell equations the homogeneous-plasma wave equation can be derived through Fourier analysis:

$$\mathbf{k} \times (\mathbf{k} \times \mathbf{E}(\mathbf{k}, \omega)) + \frac{\omega^2}{c^2} \epsilon(\mathbf{k}, \omega) \cdot \mathbf{E}(\mathbf{k}, \omega) = 0, \tag{4.1}$$

where $\mathbf{k}$ is the wave vector, $\mathbf{E}(\mathbf{k}, \omega)$ is the fluctuating electric field amplitude, ω is the wave frequency, c is the speed of light in vacuum and $\epsilon(\mathbf{k}, \omega)$ is the dielectric tensor.

Choosing the coordinates according to $\mathbf{B} = (0, 0, B)$ and $\mathbf{k} = (k_\perp, 0, k_\parallel)$, and taking the electromagnetic approximation $\mathbf{E} = (E_1, E_2, 0)$, a non-trivial solution of (4.1) must satisfy:

$$\begin{vmatrix} \frac{\omega^2}{c^2}\epsilon_{11} - k_\parallel^2 & \frac{\omega^2}{c^2}\epsilon_{12} \\ \frac{\omega^2}{c^2}\epsilon_{21} & \frac{\omega^2}{c^2}\epsilon_{22} - k^2 \end{vmatrix} = 0. \tag{4.2}$$

Given that the Hall-terms are antisymmetric $\epsilon_{12} = -\epsilon_{21}$, the characteristic equation (4.2), which is the dispersion relation, takes the form:

$$\left(\epsilon_{11} - \frac{k_\parallel^2 c^2}{\omega^2}\right)\left(\epsilon_{22} - \frac{k^2 c^2}{\omega^2}\right) + \epsilon_{12}^2 = 0. \tag{4.3}$$

The dielectric tensor can be calculated from the dielectric susceptibility contributions of the different populations of plasma particles:

$$\epsilon(\mathbf{k}, \omega) = \mathbf{I} + \sum_s \chi_s(\mathbf{k}, \omega), \tag{4.4}$$

where $\mathbf{I}$ is the dyadic unit and χ_s is the susceptibility tensor for the s population of charged particles.

By definition the susceptibility tensor can be expressed in terms of the conductivity tensor $\chi_s(\mathbf{k}, \omega) = 4\pi i \sigma_s / \omega$, and the current density determining the conductivity through Ohm's law is proportional to the first velocity moment of the distribution function $\mathbf{j}_s = q_s \int d^3v \, \mathbf{v} f_s(\mathbf{r}, \mathbf{v}, t)$. Changes of a distribution function as a result of the imposed harmonic electric field can be calculated through kinetic theory [32].

The dielectric tensor in a plasma with runaway electrons is the sum of the identity tensor and the susceptibility tensors of three different charged particle populations: that of the thermal ions (i), the thermal electrons (e) and the runaway electrons (r):

$$\epsilon(\mathbf{k}, \omega) = \mathbf{I} + \chi_i(\mathbf{k}, \omega) + \chi_e(\mathbf{k}, \omega) + \chi_r(\mathbf{k}, \omega). \tag{4.5}$$

Paper D shows that if we omit the – presumably small – effect of runaway electrons and make the assumptions $\omega_{ci} \ll \omega \ll \omega_{ce}$, $k_\perp^2 v_{Te}^2 \ll \omega^2$, $|k| \gg |k_\parallel|$ and $\omega_{pi} \ll kc \ll \omega_{pe}$, where ω_{cs} and ω_{ps} are the cyclotron and plasma frequencies for population s and v_{Te} is the electron thermal speed, we arrive at the magnetosonic-whistler dispersion relation

$$\omega_0 = k v_A \sqrt{1 + k_\parallel^2 c^2 / \omega_{pi}^2}, \tag{4.6}$$

which reduces to the magnetosonic wave $\omega_0 = k v_A$ for pure perpendicular propagation ($k_\parallel = 0$) and to the whistler wave $\omega_0 = k k_\parallel v_A^2 / \omega_{ci}$ for $k_\parallel^2 c^2 / \omega_{pi}^2 \gg 1$.

4.2 Linear stability of waves

The effect of the runaway electrons on the magnetosonic-whistler dispersion relation can be calculated using perturbative analysis, if the

density of the runaway electrons is much smaller then the density of thermal electrons. The instability growth rate for a small perturbation is

$$\gamma_i = \mathrm{Im}\delta\omega, \tag{4.7}$$

where $\delta\omega = \omega - \omega_0$, $|\delta\omega| \ll \omega_0$, with ω_0 being determined by the dispersion relation without runaway electrons (4.6).

In Paper D the linear growth rate γ_i is calculated from kinetic theory, and parameters for the most unstable wave are estimated. In a post-disruption, low temperature plasma, wave damping due to electron-ion collisions is the dominant damping mechanism, $\gamma_d = -1.5\tau_{ei}^{-1}$, where τ_{ei} is the electron-ion collision time [33]. After adding this damping to the growth rate (4.7), the instability threshold can be determined as

$$\frac{n_r}{n_e} > \frac{Z^2 B_T}{20 T_{eV}^{3/2}}, \tag{4.8}$$

where T_{eV} is the background plasma temperature in electronvolt, B_T is the magnetic field in tesla and n_r/n_e is the density fraction of runaway electrons.

The threshold (4.8) gives a critical runaway electron current density for a specified set of plasma parameters. For typical post disruption plasmas of JET ($B = 2$ T, $\mathrm{n_e} = 5 \cdot 10^{19}$ $\mathrm{m^{-3}}$, $\mathrm{T_{eV}} = 20$ eV) [34], the threshold current density is $j_r \simeq 2$ MA/m^2 for $Z = 1$, which is of the order of the observed runaway current. For ITER, the threshold is higher $j_r \simeq 12.5$ MA/m^2 due to higher magnetic field and density ($B = 5$ T, $\mathrm{n_e} = 10^{20}$ $\mathrm{m^{-3}}$).

4.3 Quasi-linear interaction of waves and fast particles

The results presented in Paper D indicate that a runaway electron beam generated in a large tokamak disruption can destabilize the whistler wave. Paper E mostly deals with the effect of the whistler wave on the distribution function of the runaway electrons.

The interaction of waves and particles can be described by the quasi-linear theory with three premises: 1. The wave amplitudes should be small enough to affect the zero-order particle orbits and distribution functions to an extent negligible for the linear theory. 2. The waves should be incoherent and have a sufficiently dense spectrum, in order

to avoid particle trapping. 3. Damping and growth rates of the waves should be small with respect to the real part of their frequencies. If all of these conditions apply, the linear theory remains valid for the rapid oscillations, and it can determine the growth rate of the instability. Effects of the wave instability on the particle distribution function can be described on a longer time scale by taking the space and time average of the Vlasov equation (3.1) for a few wave periods for all possible initial particle positions and including only the average effect of the oscillating electric field of the wave [32].

The slowly changing distribution function can be separated into two parts. One portion has a rate of evolution proportional to the spectral energy of the wave $W_k = \frac{\epsilon_0}{2}|E_k|^2$ (for a given wave polarization), where E_k is the Fourier transform of the electric field magnitude. The other part of the slowly varying distribution function has a magnitude proportional to the spectral energy of the wave. Although this later part is necessary for momentum and energy conservation, it is small and does not impose long-term changes, so it can usually be neglected [32].

The effect of the wave on the main part of the distribution function can be described as a diffusion process in the velocity space of the resonant particles. The diffusion always acts in the direction of isotropization and flattening of distribution functions, and is therefore decreasing the driving term of the instability. In the case of the relativistic runaway electron beam, the driving term for the linear wave instability is the velocity anisotropy of the runaway electron distribution function, and in Paper E it is indeed shown that the main effect of quasi-linear diffusion is the isotropization of the distribution function.

As often found in similar processes [35], the wave-particle interaction has a pulsating dynamics. The isotropization of the distribution function happens in consecutive phases accompanied by bursts of whistler waves, as the number of runaway electrons continues to grow.

If the runaway current density reaches the critical level defined in Section 4.2, and the whistler wave is destabilized, it leads to a rapid quench of the resonant part of the runaway beam, therefore the experimentally observed magnetic field threshold of $B \simeq 2$ T [14, 15] might be explained.

Chapter 5

Conclusions and outlook

The present thesis addresses two topics from the borderline of the fields of stability of waves and transport in magnetically confined fusion plasmas.

The first topic concerns the transient MHD modes observed in pure electron cyclotron heated (ECRH) discharges of the Wendelstein 7-AS (W7-AS) stellarator. These modes accompany transient ELM-like transport events, and usually last only for a few oscillations. These events have been studied by processing fluctuation and profile measurements of different diagnostics: Mirnov-coils, lithium beam emission spectroscopy (LiBES), LOTUS collective laser scattering and electron cyclotron emission spectroscopy (ECE). Aiming to recover valuable information from these transient signals, special signal processing methods have been developed based on continuous linear time-frequency transforms: the band-power correlation method and a mode number determination algorithm.

A confinement transition near the 1/3 rational edge rotational value was explored in the view of transient transport and MHD modes. It was clearly seen that transport events in 'bad' confinement conditions are more pronounced, and flattenings in the density and temperature profiles clearly correlated with the intensity of millimeter-scale turbulence and bursts of MHD modes having low poloidal mode numbers. Several parameters regarding the spatiotemporal structure and statistical correlations have been determined.

Three possible theoretical explanations of the transient MHD modes have been put forward involving drift-Alfvén turbulence, destabilization by fast electrons of ECRH or harmonic response of the plasma to a poloidally asymmetric perturbation caused by some transport event.

The choice between the alternative models should be based on simulations of the different scenarii, however, this is outside the scope of the present thesis.

The study of W7-AS data produces results that are not only relevant for the new Wendelstein-series stellarator, the W7-X being built in Greifswald, but to other fusion plasma devices, as well. The localized electromagnetic modes (LEM) seen in the TJ-II stellarator [36] resemble the transient MHD modes of W7-AS remarkably well, and similar fluctuations had been found in preliminary studies on small tokamaks also [37].

The second topic of the thesis concerns the runaway electrons generated in large tokamak disruptions. The aim is to explain experimental observations regarding the number of runaway electrons generated during a disruption. Analytical and numerical calculations based on the linear and quasi-linear kinetic theory show that the whistler wave can be destabilized due to the strong velocity anisotropy of the runaway electron distribution function, and the wave can scatter resonant electrons from the beam.

Although the results presented in this thesis show that whistler wave destabilization can play an important role, definiteness of the conclusions is limited by the simple disruption model assuming constant toroidal electric field and basically homogeneous plasma with main parameters constant in time. This could be significantly improved by including the whistler wave interaction in a self-consistent simulation of the runaway distribution function and the electric field evolution, as achieved, for instance, by the ARENA code [38].

Measurement of the whistler wave could also be attempted in disruption experiments, although these may impose heavy requirements on the plasma diagnostics. The first difficulty is that a large tokamak is necessary for the experiment, so that secondary generation would dominate. The second difficulty is the detection of ~ 10 μs long bursts of a wave having ~ 10 GHz frequency and ~ 1 mm wavelength during a disruption. Detection of the whistler wave would provide strong support for the theory.

References

[1] T.J. Dolan, Fusion Research, Pergamon Press (2000).

[2] G.M. McCracken and P. Stott, Fusion, Elsevier Academic Press (2005).

[3] I. Cook et al., Plasma Phys. Control. Fusion **44**, B121-B136 (2002).

[4] M. Wanner and the W7-X team, Plasma Phys. Control. Fusion **42**, 1179-1186 (2000).

[5] D.J. Strickler et al., Fusion Science and Technology **45**, 15 (2004).

[6] NCSX Homepage: http://ncsx.pppl.gov/

[7] The ITER team: Progress in the ITER Physics Basis, Nucl. Fusion **47** (2007).

[8] N.J. Lopes Cardozo et al., Plasma Phys. Control. Fusion **39**, B303-B316 (1997).

[9] R. Brakel and W7-AS team, Nucl. Fusion **42**, 903 (2002).

[10] M. Hirsch et al., Europhysics Conference Abstracts **22C**, 2322 (1998).

[11] S. Zoletnik et al., Phys. Plasmas **6**, 4239 (1999).

[12] P. Helander and D. J. Sigmar, Collisional Transport in Magnetized Plasmas, Cambridge University Press, Cambridge (2002).

[13] M. Lipa et al., Fusion Engineering and Design, **66-68**, 365-369 (2003).

[14] R. D. Gill, B. Alper, M. de Baar et al., Nucl. Fusion, **42**, 1039 (2002).

[15] R. Yoshino, S. Tokuda and Y. Kawano, Nucl. Fusion, **39**, 151, (2000).

[16] D. Gabor, J. Institute of Electric Engineers **93**, 429 (1946).

[17] J. Morlet, Issues in Acoustic Signal - Image Processing and Recognition, Springer-Verlag, Berlin (1983) pp. 233-262.

[18] S. Mallat, A Wavelet Tour of Signal Processing, Academic Press (2001).

[19] I.I. Orlovskiy and A.M. Kakurin, Europhysics Conference Abstracts **29C**, P1.089 (2005).

[20] MPI für Plasmaphysik, Garching: Mirnov Probes MIR-1 at W7-AS internal report (2000).

[21] M. Saffman et al., Rev. Sci. Instrum. **72**, 2579 (2001).

[22] A. Weller et al., Phys. Plasmas **8**, 931 (2001).

[23] S. Zoletnik et al., Plasma Phys. Control. Fusion **44**, 1581 (2002).

[24] M. Anton et al., J. Plasma Fusion Research SERIES **1**, 259 (1998).

[25] N.P. Basse et al., Phys. Plasmas **12**, 052512 (2005).

[26] S. Zoletnik et al., Europhysics Conference Abstracts **29C**, P-5.023 (2005).

[27] G. Papp et al., Europhysics Conference Abstracts **29C**, P-5.021 (2005).

[28] G.F. Counsell et al., Fusion Energy 2006 (Proceedings of the 21st IAEA Conference, Chengdu, 16-21 October 2006), **IAEA-CN-149**, EX/P4-6 (2006).

[29] Ya.I. Kolesnichenko et al., Phys. Plasmas **14**, 102504 (2007).

[30] H. Smith, Runaway Electrons and Alfven Eigenmodes in Tokamaks, doctoral thesis, Chalmers University of Technology, Göteborg (2006).

[31] M. N. Rosenbluth and S. V. Putvinski, Nucl. Fusion, **37**, 1355 (1977).

[32] T.H. Stix, Waves in Plasmas, American Institute of Physics, New York (1992).

[33] M. Brambilla, Phys. Plasmas, **2**, 1094 (1995).

[34] J.A. Wesson et al., Nucl. Fusion, **29**, 641 (1989).

[35] D.-I. Choi and W. Horton, Plasma Physics **20**, 903 (1977).

[36] J.A. Jiménez et al., Plasma Phys. Control. Fusion **48**, 515 (2006).

[37] S. Zoletnik, personal communication (2007).

[38] L.-G. Eriksson et al., Phys. Rev. Lett. **92**, 205004 (2004).

Included papers A–E

Paper A

G. Pokol, G. Por, S. Zoletnik, W7-AS team, "Application of a bandpower correlation method to the statistical analysis of MHD bursts in quiescent Wendelstein-7 AS stellarator plasmas", Plasma Physics and Controlled Fusion **49**, 1391-1408 (2007).

Paper B

G. Pokol, G. Por, S. Zoletnik, N. P. Basse and W7-AS team, "Amplitude correlation analysis of W7-AS Mirnov-coil array data and other transport relevant diagnostics", Proc. of 20th IAEA Fusion Energy Conference, Vilamoura, 2004, (IAEA Conference & Symposium Papers, 2005), Vol. **25/CD**, PS-EX/P6-22 (2005).

Paper C

G. Pokol, G. Papp, G. Por, S. Zoletnik, A. Weller and W7-AS team, "Experimental study and simulation of W7-AS transient MHD modes", Proc. of PLASMA 2007 International Conference on Research and Applications of Plasmas, Greifswald, 2007, (to be published in the AIP Conference Proceedings Series) TuP31 (2007).

Paper D

T. Fülöp, G. Pokol, P. Helander and M. Lisak, "Destabilization of magnetosonic-whistler waves by a relativistic runaway beam", Physics of Plasmas **13**, 062506 (2006).

Paper E

G. Pokol, T. Fülöp and M. Lisak, "Quasi-linear analysis of whistler waves driven by relativistic runaway beams in tokamaks" (to be submitted for publication)